



OPEN Improved water resources management for smart farming: a case study for Cyprus

Stelios P. Neophytides^{1,2}✉, Marinos Eliades^{1,2}, Michalis Mavrovouniotis^{1,2}, Christiana Papoutsas^{1,2}, George Papadavid³ & Diofantos G. Hadjimitsis^{1,2}

Water-scarce areas are threatened by climate crisis and, thus, there is an urgent need for optimizing water resources management. Remote sensing has been widely used for calculating the evapotranspiration over large areas, which is an essential variable for calculating the actual irrigation needs of crops. The main objective of this work is to design an approach to optimize the irrigation needs for specific crops. The island of Cyprus is used as a case study providing first insights for water management in the country. The proposed approach is crucial to the agricultural industry of Cyprus since it is located in the Mediterranean region which is affected by warm climate and drought events. Specifically, the proposed approach calculates daily the crop evapotranspiration over the island for three of the most important crops (i.e., citrus, olives, and potatoes) cultivated in Cyprus. The results of this study are showing that the three crop types are withdrawing much more water than the total annual inflow of reservoirs in 2023. Therefore, better irrigation management needs to be adopted by farmers while optimized water resources management practices have to be embraced by local authorities and stakeholders.

Keywords Evapotranspiration, Water Management, Agriculture, Climate crisis, Remote Sensing

The Mediterranean region is heavily affected by the climate crisis and has been suffering due to its dependence on irrigated agriculture¹. The island of Cyprus, as part of the eastern Mediterranean, has been characterized as a climate crisis hot spot, meaning that apart from the profound effects of temperature rise, extreme events like droughts are expected to occur more frequently than in the past century^{2,3}. Therefore, it is used as a representative case study in this work.

The utilization of agricultural water is essential since irrigated agriculture produces 40% of the world's food. In this way, agricultural productivity and consequently the international food supply are secured. An increase of at least 70% in agricultural production needs is estimated by 2050 according to TheWorldBank's reports. In particular, the increasing water scarcity currently threatens crop production in Cyprus, especially the crops which rely on irrigation inputs⁴⁻⁶. Therefore, there is an urgent need to implement sustainable irrigation in water-scarce regions under the impact of climate crisis through innovative and cost-effective solutions⁷. Cyprus agricultural land is by 20% irrigated according the TheWorldBank's annual report on 2020 (www.worldbank.org). Moreover, the Cyprus' agricultural water resources of freshwater and groundwater volumes are expected to be threatened by stresses and pressures based on future climatic scenarios⁸.

However, the mitigation (e.g., adaptation of decarbonization techniques, soil biochar enhancement, carbon sequestration, management of solar and terrestrial radiation, reduction of coal, adaptation of nature-based solutions in coastal areas and oil burn, etc.) of climate crisis can reduce the additional irrigation water requirements by 13–14%⁹⁻¹³.

The use of remote sensing techniques can have a significant contribution in improving current irrigation management practices, as they can provide crucial information on variables related to soil moisture and plant status at high spatio-temporal resolution¹⁴. In other words, remote sensing allows farmers and policymakers to improve their existing water management practices resulting in a more sustainable future for the agricultural sector in water-scarce regions such as Cyprus¹⁵.

To the best of our knowledge, dynamic satellite-based tools or services focusing on the optimization of water resources management practices in agriculture tailored for Cyprus do not exist. AgSAT¹⁶ which using similar techniques to our approach, is using forecasted weather data in contrast to our approach which is using real-time

¹ERATOSTHENES Centre of Excellence, Limassol 3012, Cyprus. ²Department of Civil Engineering and Geomatics, Cyprus University of Technology, Limassol 3012, Cyprus. ³Agricultural Research Institute, Nicosia 1516, Cyprus. ✉email: stelios.neophytides@eratosthenes.org.cy

ground-truth data. IrriSAT¹⁷ is also based on a similar approach but can be applied only for cotton cultivations and is not useful for Cyprus' agricultural industry. Thus, the aim of this work is to design an approach to support farmers on irrigation practices minimizing in this way their cost and at the same time saving water resources. The objectives of this research work are: 1) the utilization of up-to-date and near real-time data; 2) optimize water resources management according to the crop type; and 3) provide first insights for three of the most important crops in Cyprus (i.e., citrus, olives, and potatoes). The proposed approach integrates in-situ meteorological data (air temperature, humidity, wind speed), with forecasts of solar radiation derived from Copernicus Atmosphere Monitoring Centre (CAMS) for the daily calculations of evapotranspiration (*ET*), while at the same time it combines remote sensing-derived vegetation index used for deriving the coefficients of the three aforementioned crops for the daily calculations of crop-specific evapotranspiration.

Related works

ET is the process where water is returned from the earth's surface to the atmosphere in the form of water vapour. The individual components of *ET* include: a) evaporation from the soil (*E*); b) transpiration through the stomata of plants (*T*); and c) evaporation of water intercepted by the plant canopy and litter layer^{18,19}. Moreover, *ET* can provide insights for monitoring many ecological activities such as soil moisture, carbon cycle, productivity of vegetation and water budget^{20–23}.

The most accurate method to measure *ET* is using lysimeters²⁴, which are containers filled with soil covered with the crop of interest and rely on the differences in mass measurements (weighable)²⁴. However, lysimeters are costly and their installation requires lots of effort. In addition, the taken mass measurements can differ from actual field conditions (e.g., differences in root architecture, lateral and horizontal root extent).

Another way to measure *ET* is using the eddy covariance technique, which is based on the high frequency measurement of momentum, temperature, and water vapor²⁵. The basic components of the eddy covariance system are the sonic anemometer (measures three-dimensional wind speed) and the infrared gas analyzer (measures vapor concentration). The main benefit of eddy covariance is that it can provide information on *ET* over a large area^{26–28}. However, several errors may occur with the use of eddy covariance such as the contribution of vapor from areas beyond the footprint, inefficient calibrations, and errors during rainfall.

The aforementioned techniques for measuring *ET* (i.e., eddy covariance and lysimeters) cannot be implemented extensively, thus the assessment of water use patterns in irrigated crops still rely on models such as the FAO-56, which is a model that computes the actual crop evapotranspiration by multiplying the reference evapotranspiration (*ET_o*) with crop and stress coefficients adjusted for site-specific conditions¹⁸. The *ET_o* is computed from meteorological data with the use of the Penman-Monteith equation^{19,29}.

Furthermore, there are other methodologies such as the Priestley-Taylor³⁰, which is a substitute of Penman-Monteith, the Shuttleworth-Wallace³¹ which is a two-component extension of Penman-Monteith and temperature-only models like Hargreaves-Samani³² and Hamon³³. Remote sensing has also played a significant role in estimating *ET* by developing models like METRIC³⁴ and SEBAL^{35,36} or by generating ready for analysis or near-analysis products^{37–39}. For example, satellite imagery can be beneficial for making *ET* estimations at a global level because they continuously provide data about relevant biophysical parameters for long time series covering large areas⁴⁰.

Remote sensing can also help with vegetation indices correlations with crop coefficient⁴¹, such as Normalized Difference Vegetation Index (NDVI) and satellite Leaf Area Index (LAI), which are helpful in monitoring crop growth and water requirements, and adjusting them dynamically⁴². A study in the semi-arid region of Bhiwani, India showed a strong relationship between LAI and crop coefficient using a second order polynomial regression with R^2 of 0.98⁴³. An agreement analysis between NDVI and crop coefficient using ANOVA method for tomato crops showed also a great correlation through analysis conducted using Sentinel-2 images with R^2 of 0.98⁴⁴. A fourth-degree polynomial with an R^2 of 0.71 shows that LAI derived from RapidEye and Landsat 8 images can be used to estimate crop coefficient for vineyards⁴⁵. A comprehensive comparison on correlations between LAI and NDVI for estimating crop's coefficients showed a bigger error on LAI than NDVI⁴⁶.

There are applications relying on these satellite-based approaches such as AgSAT¹⁶ which is using CFSV2 gridded weather dataset within Google Earth Engine and is using Sentinel-2 NDVI and SAVI for crop coefficient estimations for various crop types such as olives, citrus, potatoes, wheat, etc. AgSAT is offered through mobile or a web-based application. IrriSAT¹⁷ is using Landsat data for calculating K_c of cotton using a generic equation and in-situ meteorological data to support the irrigation practices of cotton growers in Australia. Furthermore, IRRISAT⁴⁷ is using Landsat's LAI and in-situ meteorological data for calculating water needs based on FAO's instructions. FAO's WaPOR^{48,49} version 2 and 3 were recently released and they are offering to users annual or dekadal maps for actual evapotranspiration over the world with a resolution of 375m using VIIRS satellite. Those approaches are based on dynamic K_c using satellite variables.

On the other hand, there are other applications using conventional methodologies of water resources management. AgroClimatic Evolution⁵⁰ offers hourly *ET* calculations based on a selected meteorological station by user, information about weather conditions and time series graphs regarding *ET* and meteorological factors that are affecting the *ET*. Also, it offers other products such as evaporation, transpiration, interception, relative soil moisture, relative root zone soil moisture and net primary production. FAO's CropWat 8.0^{51,52} offers a suite of different tools for *ET* calculations, climatic data estimations, crop water requirements estimations for paddy & upland rice, daily soil water balance among others. Those calculations are made after user inputs the relevant and needed information. One other application, ETWatch⁵³ enables users to establish API calls for acquiring *ET* for their region of interest. EVAPO⁵⁴ is using meteorological data from NASA-POWER and calculates *ET* using FAO56 equation steps. A comparison between their calculations and *ET* calculated from surface stations showed a root mean square error ranging from 0.60 to 0.85⁵⁴.

Methods

Study area

Cyprus is an island situated in the eastern Mediterranean Sea (35°N , 33°W) as shown in Fig. 1, and is part of the wider area of the Eastern Mediterranean, Middle East, and North Africa region⁵⁵. The island covers a total area of 9254 km^2 and the climate is characterized as semi-arid with frequently occurring droughts. Moreover, it is observed that the climate in Cyprus has a spatio-temporal behaviour because of the different topographic characteristics arising from the mountainous terrain.

In general, Cyprus experiences hot dry summers and mild rainy winters which are typical characteristics of the Mediterranean region^{56,57}. Between years 1991 to 2020, the average mean surface temperature in Cyprus was 11.2 degrees Celsius for the winter season, 16.82 degrees Celsius for the spring season, 26.69 degrees Celsius for the summer season, and 21.03 degrees Celsius for the autumn season, according to the reports of the climate crisis in the Knowledge Portal of World Bank for 2021 [<https://climateknowledgeportal.worldbank.org/>]. Regarding precipitation amounts, the winter season had 281.06mm, spring had 90.9mm, summer had 10.3mm, and autumn had 87.81mm.

Finally, the agricultural sector of Cyprus can be divided into irrigated crops which are cultivated during the year and rain-fed cereals grown throughout the winter period. Additionally, irrigated crops in Cyprus can be separated into annual and permanent. In this study, two permanent irrigated crops (i.e., citrus and olives orchards) and one annual irrigated crop (i.e., potatoes) are considered. These crops are selected due to their high demand in water needs and their contribution in Cyprus economy.

Meteorological variables

Meteorological data for the study area were available from mid-June 2023 to the end of March 2024. The meteorological variables for the tools are collected from two different sources. At first, the meteorological variables described in Table 1 are acquired from the meteorological network [<https://www.dom.org.cy/>] of Cyprus. The network is maintained by Cyprus Department of Meteorology (DoM) and consists of 42 different automatic weather stations distributed as shown in Fig. 2. The map was created using QGIS⁵⁸ of version 3.28.3 “Firenze” [<https://blog.qgis.org/2022/10/25/qgis-3-28-firenze-is-released/>].

The stations provides measurements every 10 minutes for air temperature, wind speed, wind direction, relative humidity, and accumulated rainfall. All the collected data are automatically transmitted to the department’s database system and are validated in order to be available through an Application Programming Interface (API). Meteorological in-situ observations from the distributed weather stations shown in Fig. 2 are collected daily. The observations include the minimum temperature, maximum temperature, minimum relative humidity, maximum relative humidity and daily average wind speed.

Moreover, the solar radiation and albedo forecasted values as described in Table 1 are collected from Copernicus Atmospheric Monitoring Service (CAMS). CAMS via the Global Atmospheric Composition Forecasts services are producing forecasts twice a day consisting of more than 50 chemical species (e.g., ozone, nitrogen, dioxide, carbon monoxide), seven different types of aerosol and various meteorological variables. A



Fig. 1. Cyprus topographical map. (Source: Ikonact).

Weather variable	Unit	Range	Source
Air temperature	$^{\circ}C$	- 35/55	DoM
Relative humidity	%	0/100	DoM
Wind speed	$m \cdot s^{-1}$	0/75	DoM
Accumulated rainfall	mm	0/50	DoM
Solar radiation	$W \cdot m^{-2}$	- 1/1400	CAMS
Albedo	%	0/100	CAMS

Table 1. Description of the physical limits of the meteorological variables.

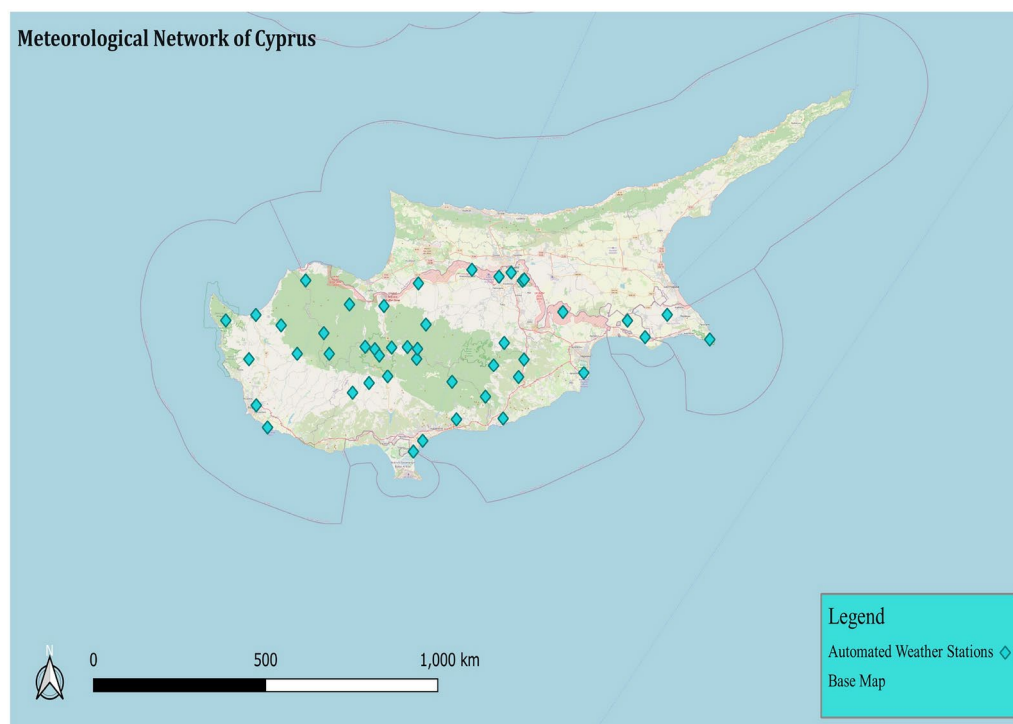


Fig. 2. Meteorological network of Cyprus. Each meteorological station is symbolized by a cyan diamond. Map created using the Free and Open Source QGIS.

process called data assimilation is taking place where initial conditions of a forecast are generated by fusing previous forecasts with space-based observations. Forecasts represent the next five days, and they are adapted to the laws of physics and chemistry to find out how much the concentrations of all species have changed over a time window.

Similar to DoM, CAMS offers an API for the collected data to be accessible. The obtained forecasted values from CAMS in combination with the aforementioned meteorological variables obtained from DoM are utilized to calculate ET_o (more details in the following subsections).

Crop labeling

The ground-truth information for the three main crop categories (i.e., citrus, olives, and potatoes) supported in this work, is gathered from the Land Parcel Identification System (LPIS) of Cyprus Agricultural Payments Organization (CAPO).

CAPO and the respective organisations of other countries maintain a geodatabase (i.e., LPIS) which contains information such as the agricultural parcel id, owner id and cultivated crop's unique code to adapt the strategies of Common Agricultural Policy related to farmers' annual subsidies. Further exploration, in future work can be considered, with an automatic crop classification using advanced Artificial Intelligence technologies. The employment of such techniques will ensure the truthiness of the crop type that is cultivated at each parcel.

Satellite variables

Satellite-based remote sensing is gathering information, using different sensors in a near-real-time basis, for multiple aspects of the environment such as vegetation, water, natural hazards and topography among others.

One of the most important variables required for the calculation of evapotranspiration is the atmospheric pressure. When it is not available as an in-situ observation from the meteorological stations, it can be calculated as a proxy of altitude. Digital Elevation Models (DEMs), produced from satellite data, are responsible to provide the information regarding the altitude. In this study the NASA's Shuttle Radar Topography Mission DEM is used which has a spatial resolution of 30m. The atmospheric pressure P_a using satellite variables is calculated as follows:

$$P_a = 101.3 \left(\frac{293 - 0.0065H}{293} \right)^{5.26}, \quad (1)$$

where H is the altitude of each meteorological station.

Another satellite variable utilized in this study is the NDVI which is a widely used and well-known spectral index calculated using the reflectance values of a target (i.e., pixel) at red and near-infrared wavelength as follows⁵⁹:

$$p_i = \frac{B8_i - B4_i}{B8_i + B4_i}, \quad (2)$$

where $B8_i$ and $B4_i$ represent the spectral reflectance at 842nm and at 665nm, respectively, for pixel i . In this work, the spectral reflectance from Sentinel-2 images is considered in which they are collected via Sentinel Hub through an API that occasionally checks for the most recent observations. Cloud and cloud shadow masking are applied to the Sentinel 2 optical images.

Specifically, the NDVI describes the vegetation greenness for an area under study as presented in Fig. 3. NDVI is useful in monitoring the phenology of a crop as well as the crop's health. The values visualized in Fig. 3 range from 0 to 1, whereas values near 0 indicate the appearance of bare soil and all the values above 0.1 characterize vegetation. Values closer to 1 correspond to dense vegetated areas. It is worth mentioning that values below 0 indicate water (e.g., oceans, lakes, and rivers) and clouds.

The mean \overline{NDVI}^k value for each parcel k is utilized to calculate the crops' coefficient and they are both stored in the application's database. \overline{NDVI}^k is calculated as follows:

$$\overline{NDVI}^k = \frac{1}{N^k} \sum_{i=0}^{N^k} p_i, \quad (3)$$

where N^k is the number of pixels within the boundaries of each agricultural parcel k and p_i are the NDVI values at the i th pixel as defined in equation (2).



Fig. 3. NDVI layer above the area of Akamas peninsula, Paphos [URL: agrinexushub.eratosthenes.org.cy].

Reference evapotranspiration

According to FAO⁶⁰, the ET_o is the evaporation power of atmosphere applied to soil and vegetation surfaces^{18,19}. The FAO Penman-Monteith method is developed by defining the reference crop as a hypothetical crop with an assumed height of 0.12m, a surface resistance of 70 s m⁻¹, and an albedo of 0.23, closely resembling the evaporation from an extensive surface of green grass of uniform height, actively growing and adequately watered.

The FAO Penman-Monteith calculates the reference evapotranspiration ($mm\ day^{-1}$) as follows:

$$ET_o = \frac{0.408\Delta(R_n - G) + \gamma \frac{900}{T+273} u_2 (e_s - e_a)}{\Delta + \gamma(1 + 0.34u_2)}, \quad (4)$$

where Δ is the slope vapour pressure curve ($kPa\ ^\circ C^{-1}$), R_n is the net radiation at the crop surface ($MJ\ m^{-2} day^{-1}$), G is the soil heat flux density ($MJ\ m^{-2} day^{-1}$), γ is the psychrometric constant ($kPa\ ^\circ C^{-1}$), T is the average daily air temperature at 2m height ($^\circ C$), u_2 is the wind speed at 2m height (ms^{-1}), e_s is the saturation vapour pressure (kPa), and e_a is the actual vapour pressure (kPa).

The slope vapour pressure Δ is calculated as follows:

$$\Delta = \frac{4098 \times \left(0.6108 \times e^{\frac{17.27 \cdot T_{avg}}{T_{avg} + 237.3}} \right)}{(T_{avg} + 237.3)^2}, \quad (5)$$

where T is the average air temperature at 2m.

The net radiation at the crop surface R_n is calculated as follows:

$$R_n = R_{ns} - R_{nl}, \quad (6)$$

where R_{ns} is the net shortwave radiation and R_{nl} is the outgoing net longwave radiation.

The soil heat flux density G is assumed to be equal to 0. In many practical applications, particularly in daily or long-term calculations, G is considered negligible in comparison to other components of the energy balance. This is because the changes in soil heat storage over a 24-hour period are minimal. Assuming $G = 0$ simplifies the calculations without significantly affecting the accuracy of the calculations.

The psychrometric constant γ is defined as follows:

$$\gamma = \frac{C_p \cdot P_a}{\epsilon \cdot \lambda}, \quad (7)$$

where C_p is the specific heat at constant pressure which is constant at 0.001013, P_a is the atmospheric pressure as calculated in equation 1, ϵ is the ratio molecular weight of water vapour/dry air which is constant at 0.622 and λ is the latent heat of vaporization which is constant at 2.45.

The average daily temperature T is defined as follows:

$$T = \frac{T_{min} + T_{max}}{2}, \quad (8)$$

where T_{min} and T_{max} is the minimum and maximum temperature calculated at each meteorological station in a day, respectively.

The saturation vapour pressure e_s is calculated as follows:

$$e_s = \frac{e_{T_{min}}^{\circ} + e_{T_{max}}^{\circ}}{2}, \quad (9)$$

where $e_{T_{min}}^{\circ}$ and $e_{T_{max}}^{\circ}$ is the minimum and maximum saturation vapour pressure at the air temperature (minimum and maximum), respectively.

The actual vapour pressure e_a is calculated as follows:

$$e_a = \frac{e_{T_{min}}^{\circ} \frac{RH_{max}}{100} + e_{T_{max}}^{\circ} \frac{RH_{min}}{100}}{2}, \quad (10)$$

where $e_{T_{min}}^{\circ}$ and $e_{T_{max}}^{\circ}$ are the minimum and maximum saturation vapour pressure at the air temperature (minimum and maximum), respectively. RH_{min} and RH_{max} are the minimum and maximum relative humidity calculated at each meteorological station in a day.

The computation steps for the ET_o are made according to the FAO-56 procedures as follows. The daily ET_o for Cyprus is calculated on a meteorological station level and then an interpolation process is executed using the Inverse Distance Weight (IDW) method to produce a daily ET_o raster over the island's territory in a resolution of 500m.

In this study, the IDW power is set to 3. The power is the parameter that let us control the influence of the known points to the interpolated values. The power is set to 2 by default. When interpolating meteorological variables using IDW, the default power value let unknown points influenced by values that are not similar to the values of the known points. On the other hand when higher power values (i.e., 4 and 5) were tested, we noticed that in mountainous areas with higher altitudes (where meteorological stations are yet not installed) the interpolated values were not representative.

Crop evapotranspiration

Understanding and addressing the dynamic water needs of crops throughout their growth stages is made possible in large part by the concept of the single crop coefficient K_c , which is essential to agricultural research and water resource management⁶¹. The K_c values linked to each stage of a crop's development from germination through vegetative growth, mid-season, and late-season phases offer vital information about the proportion of water needed at various stages of the crop's life cycle.

Due to this temporal differentiation, irrigation techniques can be precisely calibrated to provide crops with adequate quantity of water at the ideal moment for development. This relationship reflects the dynamic water requirements of crops, which is influenced by the changes in crops' canopy density throughout different growth stages. The crop coefficient of citrus, potatoes and olives are, respectively, computed with the use of the following linear equations⁶²:

$$K_c = \begin{cases} 0.10 \times \overline{NDVI}^k + 0.77, & \text{if citrus,} \\ 0.21 \times \overline{NDVI}^k + 0.64, & \text{if potatoes,} \\ -0.04 \times \overline{NDVI}^k + 0.73, & \text{if olives,} \end{cases} \quad (11)$$

where \overline{NDVI}^k is defined in equation (3).

The concept of evapotranspiration with reference to the crop coefficient was firstly introduced by Jensen⁶³, known as crop evapotranspiration ET_c . It can determine the evapotranspiration of healthy and well-fertilized crops that are growing in large agricultural parcels, and they are receiving optimal irrigation amounts. The crop evapotranspiration (ET_c) is calculated as follows:

$$ET_c = ET_o \times K_c, \quad (12)$$

where K_c is the single crop coefficient defined in equation (11) and ET_o is the reference evapotranspiration which is defined in equation (4).

The crop coefficient K_c of the crops studied in this work is calculated every 5 days at a parcel level, which is equivalent of the minimum revisiting time of Sentinel-2 whereas ET_c is calculated daily at a parcel level. In case of cloudy pixels, crop coefficient remains the same until new value occurs. Crop coefficient is calculated in 10m resolution, the same as NDVI.

Overall processing chain

The processing chain to calculate ET_c for the three investigated crops in this study (i.e., citrus, potatoes, olives) is presented in Fig. 6. First, the data collection through API calls from Cyprus DoM and CAMS service to obtain the meteorological variables, as described previously, is performed. These variables are then used by FAO56 Penman-Monteith in equation 4 to calculate ET_o at each meteorological station. Then, an interpolation using the inverse distance weight is performed to generate daily ET_o rasters.

An API call to Sentinel-Hub is executed every 5 days to acquire the recent NDVI raster. Sentinel-Hub offers access to `s2cloudless` software for creating cloud and cloud shadow masks⁶⁴. Subsequently, zonal statistics are deployed to derive mean values of NDVI and ET_o , calculated by equations (3) and (4), respectively, for each parcel that grows a particular crop in interest. NDVI is utilized to calculate dynamic crop coefficients and then ET_c is calculated. Meteorological data, NDVI values, ET_o and ET_c are stored as records in a database system. The tool is generating new data, while obtaining the required data for the different calculations from July 2023 to March of 2024.

The proposed approach in this work is enclosed as an application which is hosted in AgriNexusHub[URL: agrinexushub.eratosthenes.org.cy]. The launch page is mainly to inform users about what is offered through this web-application and agroclimatic observation tool is where all the features of the platform are concentrated



Fig. 4. Evapotranspiration layer above the area of Akrotiri, Limassol [URL: agrinexushub.eratosthenes.org.cy].

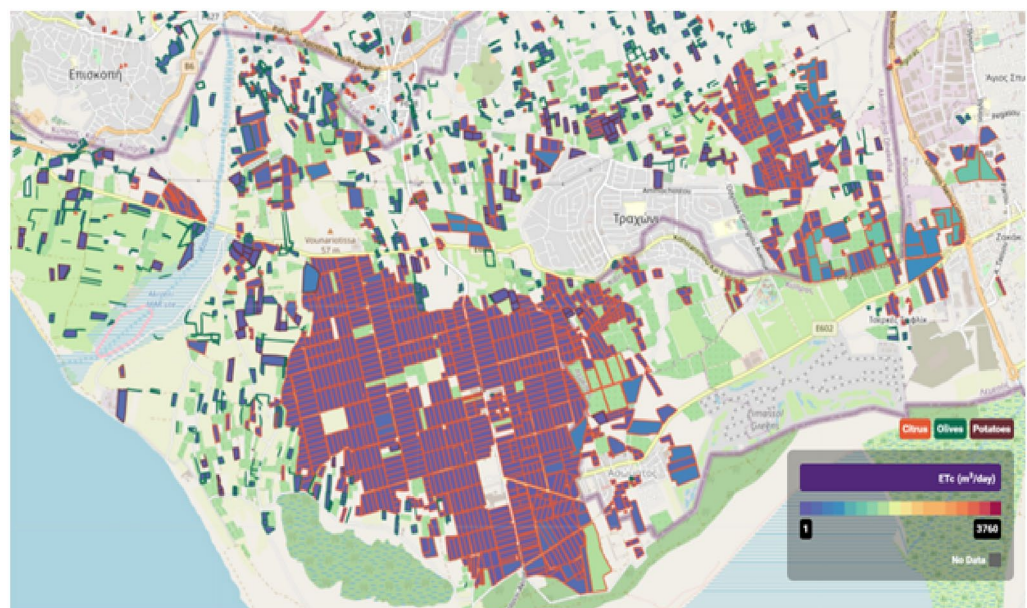


Fig. 5. Parcel-level crop evapotranspiration layer [URL: agrinexushub.eratosthenes.org.cy].

and accessible. The agroclimatic observation tool offers various features such as daily ET_o , parcel based ET_c calculations, NDVI raster and time series graphs. Figures 3, 4 and 5 are descriptive for the designed application.

Results

The collected data consists of the area average monthly ET_o , average monthly ET_c for the three crop types, and area total monthly precipitation (P). Also, the data regarding the total inflow in Cyprus water reservoirs with the information about their accumulated water capacity are gathered from Water Development Department of Cyprus.

The ratio of precipitation P to ET_o , that is $\frac{P}{ET_o}$, shows the aridity of an area during a certain season. The monthly ratio values for Cyprus from July 2023 to March 2024 are plotted in Fig. 7. In general, the characteristics of Cyprus, as a Mediterranean country, are reflected in the monthly ratios. For example, during the warmer months (i.e., July, August and September) the ratio has lower values indicating the aridity of those months

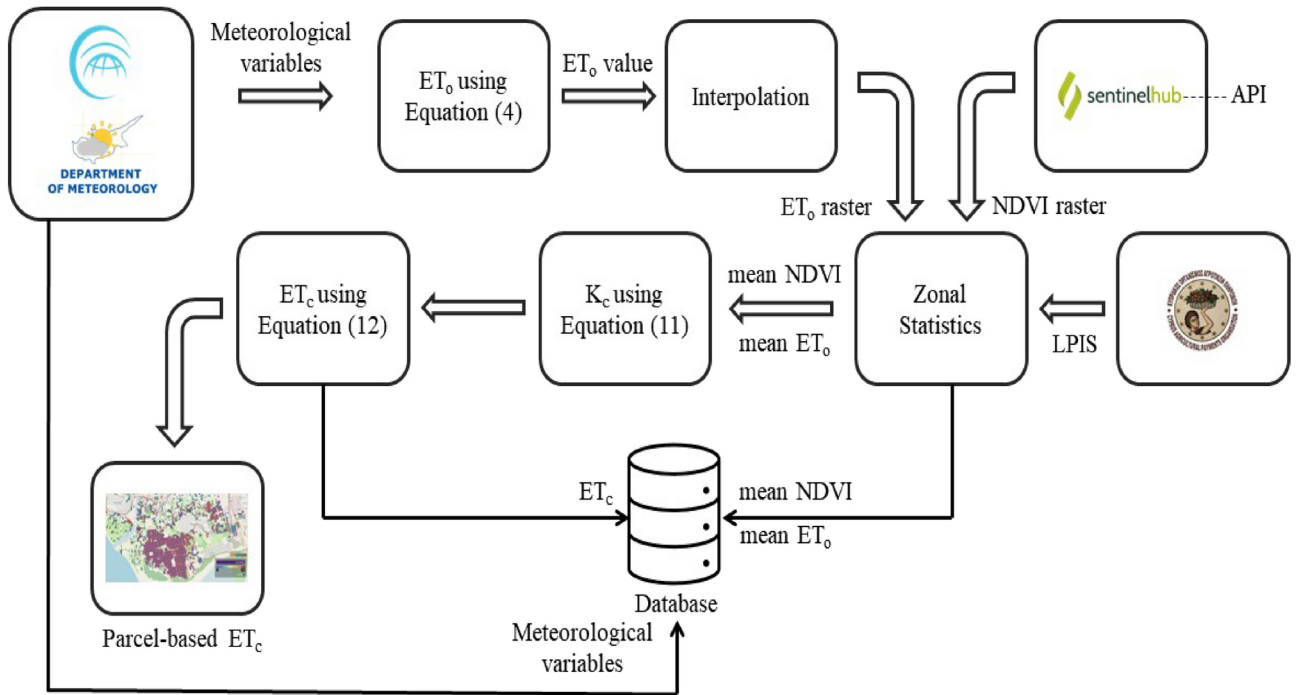


Fig. 6. Workflow diagram of the proposed tool. Double-line arrows shows the pipeline, single-line arrows shows the data storage and dashed line shows the API call to sentinelhub.

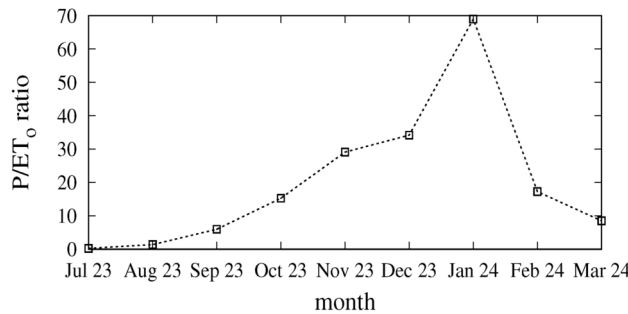


Fig. 7. P/ET_0 ratio for the whole Cyprus from July 2023 to March 2024.

whereas during the coldest months (i.e., November, December and January) the ratio has higher values indicating the humidity of the winter season.

From October 2023 to January of 2024 a gradient increase of the ratio value is noticed from approximately 20 to approximately 70, while from January to February 2024 the ratio sharply sloped from approximately 70 to approximately 15. The lowest ratio is observed for July 2023 which is approximately 0 and the highest on January 2024 which is approximately 70.

Estimation of citrus, olives, and potatoes crop evapotranspiration

The crop evapotranspiration for potatoes, olives and citrus from July 2023 to March 2024 are plotted in Fig. 8 representing their evolution in time. The results for the period of July 2023 to December 2023 show a gradual decrease of the average ET_c from approximately 12 mm/day to approximately 5 mm/day for citrus. The maximum value of ET_c for citrus orchards is decreasing from 15 mm/day to 8 mm/day, while the minimum value remains stable at approximately 6.3 mm/day except in mid-October 2023 which is decreasing to 4 mm/day. From December 2023 to February 2024, the average ET_c remains stable at lower values with fluctuations from 4 mm/day to 6 mm/day. The highest maximum ET_c during this period is 8 mm/day and the lowest minimum ET_c is approximately 3.5 mm/day. As the weather is getting warmer at the beginning of February 2024, the average ET_c is increasing from 6 mm/day to 7 mm/day and until the end of March 2024 is reaching approximately the 9 mm/day.

The average ET_c for olives during the period of July 2023 to December 2023 is gradually decreasing from approximately 11 mm/day to 5 mm/day. The maximum ET_c over this period is decreasing from approximately

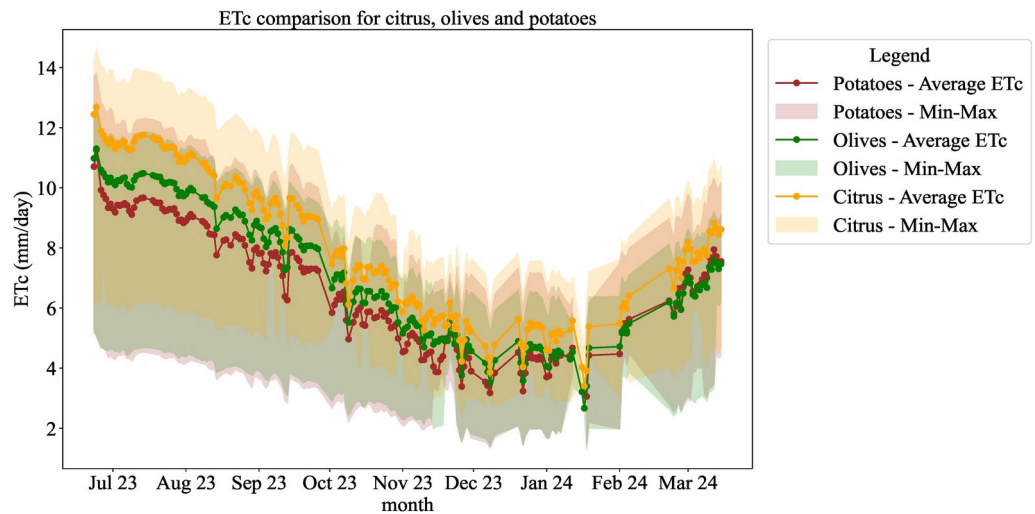


Fig. 8. Monthly ET_c comparisons for citrus, olives and potatoes. The average, minimum and maximum ET_c values are measured in millimeters per day.

Crop type	Number of parcels	Total water needs (mcm)
Citrus	8358	38.83
Olives	34561	85.93
Potatoes	5431	28.89

Table 2. Total water needs under well-watered scenarios for different crops.

13 mm/day to 8 mm/day. During the winter period (i.e., December 2023 to February 2024) the average ET_c shows a stability around 5 mm/day with some decremented picks to approximately 4 mm/day. From February to March 2024, the average ET_c is gradually increasing from approximately 5 to approximately 7 mm/day. The maximum ET_c of potatoes during the warmer period (i.e., July to September 2023) is increasing from approximately 8 mm/day to 9 mm/day, while the minimum ET_c is between approximately 2 mm/day to 6.5 mm/day.

Potatoes average ET_c at July 2023 is at approximately 11 mm/day and is steadily decreasing to about 4 mm/day on December 2023. The maximum value for potatoes is observed during June 2023 and is approximately 13.7 mm/day, while on December 2023 is decreasing to nearly 8 mm/day. Throughout the more humid period of the year (December 2023 to February 2024), the ET_c is varying from around 4 mm/day to 6 mm/day. From February 2024, where the calculated average ET_c is about 7 mm/day, it is reaching 9 mm/day by the end of March 2024, as the weather is getting hotter.

Overall, the highest average ET_c from the results is observed for citrus orchards during the whole study period, due to their high water demands. From July 2023 to mid-Jan 2024, it can be observed that olive groves has higher average ET_c value than potatoes, while higher values are observed for potatoes in the following months. In general, citrus maximum ET_c is always higher than the other two crops, while the minimum ET_c of citrus is always relatively higher. During the period of July 2023 to November 2023 it can be observed that the minimum ET_c values of potatoes are slightly lower than the olives minimum ET_c values. From December 2023 to March 2024, the minimum ET_c values are more or less similar. Similarly, from mid-January 2024, the average ET_c values of olives and potatoes are almost equal.

In summary, the highest observed ET_c values for citrus is approximately 15 mm/day, for potatoes is around 13.7 mm/day and about 12.7 mm/day for olives. The lowest ET_c for citrus is about 3 mm/day, around 2 mm/day for potatoes, and the lowest ever observed during the period is for olives, with approximately 1 mm/day.

Crop water demands

Table 2 shows the total water needs under well-watered scenarios in million cubic meters (mcm) for all parcels as calculated by ET_c classified by crop type. The total water required for the three crop categories for the period of July 2023 to end of March 2024 amounted to approximately 153.65 million cubic meters (mcm). According to the national data repository (<https://www.data.gov.cy/>) and the Water Development Department (WDD), Cyprus' dams collectively have an accumulated storage capacity of about 330 mcm. Over the past 35 years, the average annual inflow into these reservoirs has been around 83.63 mcm.

In context, the demanded water for three of the most economical valuable crops of Cyprus, during the study period is almost half of the total reservoir capacity and specifically is accounting for 46.5% of the available

accumulated dams' capacity. This substantial water requirement places a significant strain on available resources, emphasizing the intensive nature of agricultural water use.

Moreover, the water needs of the three crops is notably higher than the average annual inflow. More specifically, citrus, olives and potatoes required 84% more water than the average yearly inflow into the water reservoirs. To be more precise, the actual inflow during the period was 21.59 mcm, as Cyprus suffered from a dry winter. In comparison, the crops needed approximately 612% more water than the accumulated inflow. This discrepancy underlines the high pressure of agricultural water needs to Cyprus' water resources, and highlights the urgent need for optimized management in different practices like irrigation scheduling, irrigation appliance, groundwater sustainability and aquifer recharge.

It is noted that the tool is calculating crop evapotranspiration which corresponds to water needs assuming well-watered scenarios in the agricultural industry and the farming environments. Furthermore, it is expected that the calculations of the actual evapotranspiration will be lower and so on, the total water requirements.

Discussion

Future climatic projection shows an overall increase in water scarcity over the Eastern Mediterranean region, including the island of Cyprus^{8,65}. Thus, there is an urgent need to implement smart farming in water scarce regions, especially in the context of climate crisis. Our approach relies on the use of K_c based on the FAO56 principles. FAO's Aquastat relies on standard K_c values, which are assigned for each crop growth stage (i.e., initial stage, mid-season and at harvesting or end season). The advantage of these segmented K_c values is that it requires the knowledge of only three values. However, these K_c values can deviate from the tabulated values due to different planting densities and agronomic practices^{6,66}. In our calculations a dynamic crop coefficient based on the satellite NDVI is considered which gives a different perspective than other approaches.

In Table 3 below the differences between the aforementioned existing applications (i.e., AgroClimatic Evolution⁵⁰ (ACE), FAO's WaPOR^{48,49} (WPR), FAO's CropWat^{51,52} (FCW), ETWatch⁵³ (ETW), EVAPO⁵⁴ (EVP), AgSAT¹⁶ (AGS), IrriSAT¹⁷ (IST), and IRRISAT⁴⁷ (IRT)) in comparison to ours are described. All the applications are compared for their *spatial resolution* which corresponds to products with resolution lower than 500m, *temporal resolution* which describes products that offer at least daily calculations. It is also important to compare applications in terms of calculating *water needs*. This comparison implies also if applications are integrating or using *in-situ data*, if the water needs calculations are *crop specific* which shows the inflexibility of an approach to adapt in other crops, supporting *multiple crops* and if they are *user-friendly* from farmer's side.

ACE and FCW lacks in terms of spatial resolution which means that significant information is lost in their calculations. WPR, AGS and IRT do not offer information on a daily basis. Thus, these applications are not practical for irrigation management. The provided calculations from ACE, ETW and EVP do not meet the requirements for water needs calculations. WPR, ETW, EVP and AGS are not using in-situ data from meteorological stations meaning that the accuracy of the evapotranspiration calculations is not sufficient. From the compared application, only IRT is flexible to calculate evapotranspiration for multiple crops. ETW and IST are crop specific which shows their rigidity to adapt in calculations for other crop types. Finally, FCW and ETW are not user friendly and, thus, cannot be easily used from farmers (users) for their daily practices.

The proposed system offers daily water need calculations for different crop types, specific to their growth stages combining satellite and in-situ data. Furthermore, offers its product in a spatial resolution of 500m. Finally, it worth mentioning that the proposed system does not consider the topographical details of the areas because the IDW interpolation method is used. However, since the Cyprus has a dense meteorological network the ET_o estimates are reliable. In fact, since our approach is based on ET_c estimations, which assumes unlimited water availability, any deviations between a dry and wet year is not expected for the estimated parameters. However, it should be highlighted that the Mediterranean region often experiences extended dry periods contrary to the assumption made above. Due to limited available data the current study is not considering estimations of crop evapotranspiration on extended dry periods.

Conclusions

The ratio of P and ET_o calculations were as expected, indicating arid summer season and humid winter season. The aridity of the summer period rises the optimization of water resources management in Cyprus especially for the agricultural sector. Moreover, the evolution of ET_c in the study period, indicates the high crop water demands, especially the intense water needs of citrus.

Feature	ACE	WPR	FCW	ETW	EVP	AGS	IST	IRT	Ours
Spatial resolution		✓		✓	✓	✓	✓	✓	✓
Temporal resolution	✓		✓	✓	✓		✓		✓
Water needs calculations		✓	✓			✓	✓	✓	✓
In-situ data	✓		✓				✓	✓	✓
Multiple crops								✓	✓
Crop specific				✓			✓		
User experience	✓	✓			✓	✓	✓	✓	✓

Table 3. Comparison of different agricultural and irrigation management tools. The symbol ✓ indicates if a feature is contained in each application.

According to the results of our proposed approach, during the period of July 2023 to end of March 2024, 612% more water is required, based on ET_c which assumes well-watered scenario, from three of the most economic valuable crops of Cyprus, underscoring a critical imbalance between available water supply and demand. This study highlights the critical water resource challenges that the Cyprus agricultural industry is currently facing. Our approach enclosed in an application, is the first step to fill the gap of a water resources observatory in Cyprus.

The main limitation of this study is the lack of data over an extended period. Therefore, in our study the estimations of crop evapotranspiration are based on a short period.

In the future, calculations of the actual evapotranspiration and the combination with in-situ soil moisture sensors and the use of novel technologies will fill more of this gap and help agricultural industry to reach the sustainability upon climate crisis. Moreover, our future studies will consider longer periods to further validate our estimations. Through the described application, there is a high potential for the development of an irrigation management application, in order to help farmers produce more yield with less water and potentially vanish the future threats of the agricultural industry in the Mediterranean region and the neighbour countries. Another future direction is to use the approach to the rest of the Eastern Mediterranean, Middle East, and North Africa region.

Data availability

Data are provided upon reasonable request. Contact corresponding author at stelios.neophytides@eratosthenes.org.cy.

Received: 26 August 2024; Accepted: 9 December 2024

Published online: 30 December 2024

References

- Fader, M., Shi, S., Von Bloh, W., Bondeau, A. & Cramer, W. Mediterranean irrigation under climate change: more efficient irrigation needed to compensate for increases in irrigation water requirements. *Hydrol. Earth Syst. Sci.* **20**, 953–973. <https://doi.org/10.5194/hess-20-953-2016> (2016).
- Döll, P. Impact of climate change and variability on irrigation requirements: A global perspective. *Clim. Change* **54**, 269–293. <https://doi.org/10.1023/A:1016124032231> (2002).
- Zittis, G. et al. Climate Change and Weather Extremes in the Eastern Mediterranean and Middle East. *Rev. Geophys.* **60**, e2021RG000762. <https://doi.org/10.1029/2021RG000762> (2022).
- Adamides, G. A review of climate-smart agriculture applications in cyprus. *Atmosphere* **11**, 898. <https://doi.org/10.3390/atmos11090898> (2020).
- Adamides, G. et al. Smart farming techniques for climate change adaptation in cyprus. *Atmosphere* **11**, 557. <https://doi.org/10.3390/atmos11060557> (2020).
- Eliades, M., Bruggeman, A., Djuma, H., Christofi, C. & Kuells, C. Quantifying Evapotranspiration and Drainage Losses in a Semi-Arid Nectarine (*Prunus persica* var. *nucipersica*) Field with a Dynamic Crop Coefficient (Kc) Derived from Leaf Area Index Measurements. *Water* **14**, 734. <https://doi.org/10.3390/w14050734> (2022).
- Nikolaou, G., Neocleous, D., Christou, A., Kitta, E. & Katsoulas, N. Implementing sustainable irrigation in water-scarce regions under the impact of climate change. *Agronomy* **10**, 1120. <https://doi.org/10.3390/agronomy10081120> (2020).
- Papadopoulou, M. P. et al. Agricultural water vulnerability under climate change in cyprus. *Atmosphere* **11** (2020).
- Fawzy, S., Osman, A. I., Doran, J. & Rooney, D. W. Strategies for mitigation of climate change: A review. *Environ. Chem. Lett.* **18**, 2069–2094. <https://doi.org/10.1007/s10311-020-01059-w> (2020).
- Fischer, G., Tubiello, F. N., Van Velthuizen, H. & Wiberg, D. A. Climate change impacts on irrigation water requirements: Effects of mitigation, 1990–2080. *Technol. Forecast. Soc. Chang.* **74**, 1083–1107. <https://doi.org/10.1016/j.techfore.2006.05.021> (2007).
- VijayaVenkataRaman, S., Iniyan, S. & Goic, R. A review of climate change, mitigation and adaptation. *Renew. Sustain. Energy Rev.* **16**, 878–897. <https://doi.org/10.1016/j.rser.2011.09.009> (2012).
- Panagiotou, C. F., Stefan, C., Papanastasiou, P. & Sprenger, C. Quantitative microbial risk assessment (QMRA) for setting health-based performance targets during soil aquifer treatment. *Environ. Sci. Pollut. Res.* **30**, 14424–14438. <https://doi.org/10.1007/s11356-022-22729-y> (2023).
- Stylianou, M. et al. Assessing the influence of biochars on the hydraulic properties of a loamy sand soil. *Biomass Convers. Biorefinery* **11**, 315–323. <https://doi.org/10.1007/s13399-020-01114-0> (2021).
- Foster, T., Mieno, T. & Brozović, N. Satellite-based monitoring of irrigation water use: assessing measurement errors and their implications for agricultural water management policy. *Water Resour. Res.* **56**, e2020WR028378. <https://doi.org/10.1029/2020WR028378> (2020).
- Christou, A., Dalias, P. & Neocleous, D. Spatial and temporal variations in evapotranspiration and net water requirements of typical Mediterranean crops on the island of Cyprus. *J. Agric. Sci.* **155**, 1311–1323. <https://doi.org/10.1017/S0021859617000405> (2017).
- Jaafar, H., Mourad, R., Hazimeh, R. & Sujud, L. AgSAT: A smart irrigation application for field-scale daily crop ET and water requirements using satellite imagery. *Remote Sensing* **14**, 5090. <https://doi.org/10.3390/rs14205090> (2022).
- Hornbuckle, J., Montgomery, J., Hume, I. H. & Vleeshouwer, J. Irrisat - weather based scheduling and benchmarking technology. In: Proc. 17th ASA Conference (2015).
- Allen, R. G., Pereira, L. S., Raes, D., Smith, M. & others. Crop evapotranspiration—Guidelines for computing crop water requirements—FAO Irrigation and drainage paper 56. Fao, Rome **300**, D05109 (1998).
- Pereira, L. S., Allen, R. G., Smith, M. & Raes, D. Crop evapotranspiration estimation with FAO56: Past and future. *Agric. Water Manag.* **147**, 4–20. <https://doi.org/10.1016/j.agwat.2014.07.031> (2015).
- He, L., Chen, Y. & Li, J. A three-level framework for balancing the tradeoffs among the energy, water, and air-emission implications within the life-cycle shale gas supply chains. *Resour. Conserv. Recycl.* **133**, 206–228. <https://doi.org/10.1016/j.resconrec.2018.02.015> (2018).
- Siakou, M. et al. Effects of deficit irrigation on ‘Koroneiki’ olive tree growth, physiology and olive oil quality at different harvest dates. *Agric. Water Manag.* **258**, 107200. <https://doi.org/10.1016/j.agwat.2021.107200> (2021).
- Verstraeten, W., Veroustraete, F. & Feyen, J. Assessment of evapotranspiration and soil moisture content across different scales of observation. *Sensors* **8**, 70–117. <https://doi.org/10.3390/s8010070> (2008).
- Yuan, W. et al. Global estimates of evapotranspiration and gross primary production based on MODIS and global meteorology data. *Remote Sens. Environ.* **114**, 1416–1431. <https://doi.org/10.1016/j.rse.2010.01.022> (2010).

24. Fank, J. Lysimeters: a tool for measurements of soil fluxes. Publication Title: Encyclopedia of Agrophysics. Pages: 428–431, (2011).
25. Kool, D. et al. A review of approaches for evapotranspiration partitioning. *Agric. For. Meteorol.* **184**, 56–70. <https://doi.org/10.1016/j.agrformet.2013.09.003> (2014).
26. Feng, X. et al. Quantifying winter wheat evapotranspiration and crop coefficients under sprinkler irrigation using eddy covariance technology in the North China Plain. *Agric. Water Manag.* **277**, 108131. <https://doi.org/10.1016/j.agwat.2022.108131> (2023).
27. Liu, B. et al. Comparison of evapotranspiration measurements between eddy covariance and lysimeters in paddy fields under alternate wetting and drying irrigation. *Paddy Water Environ.* **17**, 725–739. <https://doi.org/10.1007/s10333-019-00753-y> (2019).
28. Rafi, Z. et al. Partitioning evapotranspiration of a drip-irrigated wheat crop: Inter-comparing eddy covariance-, sap flow-, lysimeter- and FAO-based methods. *Agric. For. Meteorol.* **265**, 310–326. <https://doi.org/10.1016/j.agrformet.2018.11.031> (2019).
29. Zotarelli, L., Dukes, M. D., Romero, C. C., Migliaccio, K. W. & Morgan, K. T. Step by step calculation of the penman-monteith evapotranspiration (fao-56 method). EDIS (2024).
30. Pereira, A. R. The Priestley-Taylor parameter and the decoupling factor for estimating reference evapotranspiration. *Agric. For. Meteorol.* **125**, 305–313. <https://doi.org/10.1016/j.agrformet.2004.04.002> (2004).
31. Brisson, N., Itier, B., L'Hotel, J. C. & Lorendeau, J. Y. Parameterisation of the Shuttleworth-Wallace model to estimate daily maximum transpiration for use in crop models. *Ecol. Model.* **107**, 159–169. [https://doi.org/10.1016/S0304-3800\(97\)00215-9](https://doi.org/10.1016/S0304-3800(97)00215-9) (1998).
32. Hargreaves, G. H. & Samani, Z. A. Estimating potential evapotranspiration. *J. Irrigat. Drain. Div.* **108**, 225–230. <https://doi.org/10.1061/JRCEA4.0001390> (1982).
33. Hamon, W. R. Estimating potential evapotranspiration. *J. Hydraul. Div.* **87**, 107–120. <https://doi.org/10.1061/JYCEAJ.0000599> (1961).
34. Mondal, I., Thakur, S., De, A. & De, T. K. Application of the METRIC model for mapping evapotranspiration over the Sundarban Biosphere Reserve, India. *Ecol. Indic.* **136**, 108553. <https://doi.org/10.1016/j.ecolind.2022.108553> (2022).
35. Bastiaanssen, W., Menenti, M., Feddes, R. & Holtlag, A. A remote sensing surface energy balance algorithm for land (SEBAL). 1. Formulation. *J. Hydrol.* **212–213**, 198–212. [https://doi.org/10.1016/S0022-1694\(98\)00253-4](https://doi.org/10.1016/S0022-1694(98)00253-4) (1998).
36. Bastiaanssen, W. G. M. et al. SEBAL model with remotely sensed data to improve water-resources management under actual field conditions. *J. Irrig. Drain. Eng.* **131**, 85–93. [https://doi.org/10.1061/\(ASCE\)0733-9437\(2005\)131:1\(85\)](https://doi.org/10.1061/(ASCE)0733-9437(2005)131:1(85)) (2005).
37. Bai, P. Comparison of remote sensing evapotranspiration models: Consistency, merits, and pitfalls. *J. Hydrol.* **617**, 128856. <https://doi.org/10.1016/j.jhydrol.2022.128856> (2023).
38. Mu, Q., Heinsch, F. A., Zhao, M. & Running, S. W. Development of a global evapotranspiration algorithm based on MODIS and global meteorology data. *Remote Sens. Environ.* **111**, 519–536. <https://doi.org/10.1016/j.rse.2007.04.015> (2007).
39. Zhang, K. et al. Parameter analysis and estimates for the MODIS evapotranspiration algorithm and multiscale verification. *Water Resour. Res.* **55**, 2211–2231. <https://doi.org/10.1029/2018WR023485> (2019).
40. Pan, S. et al. Evaluation of global terrestrial evapotranspiration using state-of-the-art approaches in remote sensing, machine learning and land surface modeling. *Hydrol. Earth Syst. Sci.* **24**, 1485–1509. <https://doi.org/10.5194/hess-24-1485-2020> (2020).
41. Mokhtari, A. et al. Calculating potential evapotranspiration and single crop coefficient based on energy balance equation using Landsat 8 and Sentinel-2. *ISPRS J. Photogramm. Remote. Sens.* **154**, 231–245. <https://doi.org/10.1016/j.isprsjprs.2019.06.011> (2019).
42. Pôças, I., Calera, A., Campos, I. & Cunha, M. Remote sensing for estimating and mapping single and basal crop coefficients: A review on spectral vegetation indices approaches. *Agric. Water Manag.* **233**, 106081. <https://doi.org/10.1016/j.agwat.2020.106081> (2020).
43. Singh Rawat, K., Kumar Singh, S., Bala, A. & Szabó, S. Estimation of crop evapotranspiration through spatial distributed crop coefficient in a semi-arid environment. *Agric. Water Manag.* **213**, 922–933. <https://doi.org/10.1016/j.agwat.2018.12.002> (2019).
44. Ihuoma, S., Madramootoo, C. & Kalacska, M. Integration of satellite imagery and in situ soil moisture data for estimating irrigation water requirements. *Int. J. Appl. Earth Obs. Geoinf.* **102**, 102396. <https://doi.org/10.1016/j.jag.2021.102396> (2021).
45. Vanino, S. et al. Estimation of evapotranspiration and crop coefficients of tendone vineyards using multi-sensor remote sensing data in a Mediterranean environment. *Remote Sensing* **7**, 14708–14730. <https://doi.org/10.3390/rs71114708> (2015).
46. Duchemin, B. et al. Monitoring wheat phenology and irrigation in Central Morocco: On the use of relationships between evapotranspiration, crops coefficients, leaf area index and remotely-sensed vegetation indices. *Agric. Water Manag.* **79**, 1–27. <https://doi.org/10.1016/j.agwat.2005.02.013> (2006).
47. Urso, G. D., Michele, C. D. & Bolognesi, S. F. IRRISAT: the Italian On-line Satellite Irrigation Advisory Service. In EFITA-WCCA-CIGR Conference in Sustainable Agriculture through ICT Innovation (2013).
48. Geshnigani, F. S., Mirabbasi, R. & Golabi, M. R. Evaluation of FAO's WaPOR product in estimating the reference evapotranspiration for stream flow modeling. *Theoret. Appl. Climatol.* **144**, 191–201. <https://doi.org/10.1007/s00704-021-03534-y> (2021).
49. Blatchford, M. L. et al. Evaluation of WaPOR V2 evapotranspiration products across Africa. *Hydrol. Process.* **34**, 3200–3221. <https://doi.org/10.1002/hyp.13791> (2020).
50. Soler-Méndez, M., Parras-Burgos, D., Benouna-Bennouna, R. & Molina-Martínez, J. M. Agroclimatic Evolution web application as a powerful solution for managing climate data. *Sci. Rep.* **12**, 6716. <https://doi.org/10.1038/s41598-022-10316-7> (2022).
51. Gabr, M.E.-S. Management of irrigation requirements using FAO-CROPWAT 8.0 model: A case study of Egypt. *Model. Earth Syst. Environ.* **8**, 3127–3142. <https://doi.org/10.1007/s40808-021-01268-4> (2022).
52. Vozzhova, R. A. et al. Assessment of the CROPWAT 8.0 software reliability for evapotranspiration and crop water requirements calculations. *J. Water Land Dev.* **39**, 147–152. <https://doi.org/10.2478/jwld-2018-0070> (2018).
53. Wu, F. et al. ETWatch cloud: APIs for regional actual evapotranspiration data generation. *Environ. Model. Softw.* **145**, 105174. <https://doi.org/10.1016/j.envsoft.2021.105174> (2021).
54. Maldonado, W., Valeriano, T. T. B. & De Souza Rolim, G. EVAPO: A smartphone application to estimate potential evapotranspiration using cloud gridded meteorological data from NASA-POWER system. *Comput. Electron. Agric.* **156**, 187–192. <https://doi.org/10.1016/j.compag.2018.10.032> (2019).
55. Eliades, M. et al. Earth observation in the emmena region: Scoping review of current applications and knowledge gaps. *Remote Sens.* [SPACE] <https://doi.org/10.3390/rs15174202> (2023).
56. Giannakopoulos, C., Hadjinicolaou, P., Kostopoulou, E., Varotsos, K. V. & Zerefos, C. Precipitation and temperature regime over Cyprus as a result of global climate change. *Adv. Geosci.* **23**, 17–24. <https://doi.org/10.5194/adgeo-23-17-2010> (2010).
57. Hadjinicolaou, P. et al. Mid-21st century climate and weather extremes in Cyprus as projected by six regional climate models. *Reg. Environ. Change* **11**, 441–457. <https://doi.org/10.1007/s10013-010-0153-1> (2011).
58. QGIS Development Team. QGIS Geographic Information System. QGIS Association (2024).
59. Huang, S., Tang, L., Hupy, J. P., Wang, Y. & Shao, G. A commentary review on the use of normalized difference vegetation index (NDVI) in the era of popular remote sensing. *J. For. Res.* **32**, 1–6. <https://doi.org/10.1007/s11676-020-01155-1> (2021).
60. Allan, R., Pereira, L. & Smith, M. Crop evapotranspiration-Guidelines for computing crop water requirements-FAO Irrigation and drainage paper 56, vol. 56 (1998).
61. Guerra, E., Ventura, F. & Snyder, R. L. Crop Coefficients: A Literature Review. *J. Irrig. Drain. Eng.* **142**, 06015006. [https://doi.org/10.1061/\(ASCE\)IR.1943-4774.0000983](https://doi.org/10.1061/(ASCE)IR.1943-4774.0000983) (2016).
62. Mahmoud, S. H. & Gan, T. Y. Irrigation water management in arid regions of Middle East: Assessing spatio-temporal variation of actual evapotranspiration through remote sensing techniques and meteorological data. *Agric. Water Manag.* **212**, 35–47. <https://doi.org/10.1016/j.agwat.2018.08.040> (2019).

63. Jensen, M. E. *Water Consumption by Agricultural Plants (Chapter1)* (Academic Press, 1968).
64. Braaten, J. Sentinel-2 cloud masking with s2cloudless. GitHub repository (2022).
65. Chenoweth, J. et al. Impact of climate change on the water resources of the eastern mediterranean and middle east region: Modeled 21st century changes and implications. *Water Resour. Res.*[SPACE]<https://doi.org/10.1029/2010WR010269> (2011).
66. Pereira, L. et al. Prediction of crop coefficients from fraction of ground cover and height. Background and validation using ground and remote sensing data. *Agricultural Water Management* **241**, 106197. <https://doi.org/10.1016/j.agwat.2020.106197> (2020).

Acknowledgements

The authors acknowledge the 'EXCELSIOR': ERATOSTHENES: Excellence Research Centre for Earth Surveillance and Space-Based Monitoring of the Environment H2020 Widespread Teaming project (www.excelsior2020.eu). The 'EXCELSIOR' project has received funding from the European Union's Horizon 2020 research and innovation programme under Grant Agreement No 857510, from the Government of the Republic of Cyprus through the Directorate General for the European Programmes, Coordination and Development and the Cyprus University of Technology. This paper is partially supported by the European Union's HORIZON Research and Innovation Programme under grant agreement No 101120657, project ENFIELD (European Lighthouse to Manifest Trustworthy and Green AI).

Author contributions

Conceptualization: S.P.N., M.E. and M.M.; Data analysis: S.P.N., M.E. and M.M.; Data collection: C.P. and G.P.; Writing-original draft preparation: S.P.N., M.E. and M.M.; Review and editing: D.G.H., M.M. and M.E.

Declarations

Competing interests

The authors declare no competing interests.

Additional information

Correspondence and requests for materials should be addressed to S.P.N.

Reprints and permissions information is available at www.nature.com/reprints.

Publisher's note Springer Nature remains neutral with regard to jurisdictional claims in published maps and institutional affiliations.

Open Access This article is licensed under a Creative Commons Attribution-NonCommercial-NoDerivatives 4.0 International License, which permits any non-commercial use, sharing, distribution and reproduction in any medium or format, as long as you give appropriate credit to the original author(s) and the source, provide a link to the Creative Commons licence, and indicate if you modified the licensed material. You do not have permission under this licence to share adapted material derived from this article or parts of it. The images or other third party material in this article are included in the article's Creative Commons licence, unless indicated otherwise in a credit line to the material. If material is not included in the article's Creative Commons licence and your intended use is not permitted by statutory regulation or exceeds the permitted use, you will need to obtain permission directly from the copyright holder. To view a copy of this licence, visit <http://creativecommons.org/licenses/by-nc-nd/4.0/>.

© The Author(s) 2024